CrystEngComm

PAPER

View Article Online
View Journal | View Issue

Cite this: *CrystEngComm*, 2015, **17**, 8339

Surface-step-terrace tuned magnetic properties of epitaxial $LaBaCo_2O_{5.5+\delta}$ thin films on vicinal (La,Sr)(Al,Ta)O_3 substrates

Ming Liu,*[a] Shengping Ren,[a] Jiangbo Lu,[a] Chunrui Ma,[b] Xing Xu[c] and Chonglin Chen*[cd]

Received 6th August 2015,
Accepted 28th September 2015

DOI: 10.1039/c5ce01575h

www.rsc.org/crystengcomm

Interface-engineered double-perovskite structural $LaBaCo_2O_{5.5+\delta}$ thin films were highly epitaxially fabricated on (001) (La,Sr)(Al,Ta)O_3 substrates with various miscut angles of 0°, 1°, 3° and 5° using a pulsed laser deposition system. All the $LaBaCo_2O_{5.5+\delta}$ thin films have a *c*-axis orientation with a highly epitaxial crystalline quality. Moreover, the effect of the interface tuning mechanism on the magnetic properties has been systematically investigated using physical properties measurement systems. Larger strain can be obtained by increasing the substrates' surface miscut angles and can further enhance the magnetic properties of the $LaBaCo_2O_{5.5+\delta}$ thin films. All these results reveal that interface engineering using surface-step-terraces is an effective way of tuning/controlling the magnetic properties of $LaBaCo_2O_{5.5+\delta}$ films.

Introduction

Transition metal oxides (TMOs) have received considerable research attention from scientists and technicians in the last few decades due to the new physical properties in this area, such as colossal magneto-resistivity, superconductivity and use as a memristor.[1–6] Especially, cobaltate oxides have been intensively studied recently due to their many unique physical properties in magnetics, electronics and optics, which result from the strong correlations and interactions of the charge, orbitals, spin and photons.[7–9] Among them, the double perovskite cobaltate systems with the formula of $RACo_2O_{5.5+\delta}$ (R = rare earth ion, A = Sr, Ca, Ba) exhibit mixed valence states of Co ions ($Co^{2+}/Co^{3+}/Co^{4+}$), various spin-state configurations, giant magnetoresistance effects and excellent catalytic behavior *etc.*[10–14] Research into these systems not only explores their complex magnetic ground states and the relationship with the Co spin-state transition at low temperatures but also the mechanism of the remarkable mixed conductivity and catalytic properties at high temperatures, and their excellent physical properties can be used to design various kinds of new concept devices, such as energy harvesters, electrical and chemical sensors, *etc.* Among them, $LaBaCo_2O_{5.5+\delta}$ (LBCO) cobaltate systems with three various phase structures of A-site order, nano-area order and disorder have shown many unique physical properties and phenomena.[15–19] In order to further investigate the physical properties in such complex cobaltate systems, single crystalline thin films are critically desired. In our previous work, highly epitaxial single crystalline LBCO thin films have been fabricated and these films possess an extraordinary sensitivity to reducing/oxidizing environments at high temperatures and excite a much larger magnetoresistance value than those from the various phases of the bulk material at low temperatures.[20–24]

Interface engineering is becoming increasingly important in tuning/controlling the microstructures and physical properties of advanced multifunctional complex oxide thin films and nano-scale materials, which can be used to achieve novel electrical, magnetic and optical properties, *etc.*[25–30] For epitaxial thin films, controlling the interface structure between the grown film and the substrate can effectively tune the interface strain and further modify the physical properties.[31–33] Normally, the interface strain can be tuned by choosing the lattice mismatch between the films and substrates or controlling the thickness of the films. Recently, Chen *et al.* reported a model in detail that shows that the "local strain" resulting from the substrate-surface-terrace can effectively tune its epitaxial nature and physical properties, such as various anti-phase domain boundary structures, and surface-step-terrace-induced strain.[34] Normally, lots of surface-step-terraces exist on the surfaces of single crystals, which cannot match an exact number of unit cells or atomic planes in the deposited film. The mismatch between the film and the substrate terrace will

[a] *Electronic Materials Research Laboratory, Key Laboratory of the Ministry of Education & International Center for Dielectric Research, Xi'an Jiaotong University, Xi'an 710049, PR China. E-mail: m.liu@mail.xjtu.edu.cn*
[b] *State Key Laboratory for Mechanical Behavior of Materials, Xi'an Jiaotong University, Xi'an 710049, People's Republic of China*
[c] *Department of Physics and Astronomy, University of Texas at San Antonio, TX 78249, USA. E-mail: cl.chen@utsa.edu*
[d] *The Texas Center for Superconductivity, University of Houston, TX 77004, USA*

result in an additional strain energy, which cannot be released *via* edge dislocations and will be stored in the films. The stored strain energy in the films will significantly alter their microstructures and physical properties.

In this study, we systematically investigate the effect of the surface-step-terrace tuning mechanism on the magnetic properties of LBCO epitaxial thin films on (001) vicinal (La,Sr)(Al, Ta)O_3 (LSAT) substrates. All these films have an excellent epitaxial crystalline quality. The strain states have been directly obtained using reciprocal space mapping technology, which revealed that the interface strain can be tuned by the surface-step-terrace. Moreover, the strain states can further modify the magnetic properties of the LBCO thin films. It is revealed that interface engineering using surface-step-terraces is an effective method to tune/control the interface strain and physical properties of LBCO thin films.

Experimental

Highly epitaxial LBCO thin films with a (001) orientation were grown on vicinal (001) (LSAT) single-crystalline substrates with various miscut angles of 0°, 1°, 3° and 5° using a KrF excimer pulsed laser deposition system with a wavelength of 248 nm. The single-crystal LSAT substrates have been used to grow LFO films, which have a relatively small lattice mismatch (~0.5%) with lithium ferrite materials (MAO substrate: a ~ 3.868 Å; LBCO bulk material: a ~ 3.886 Å). Before the film growth, the base pressure of the pulsed laser

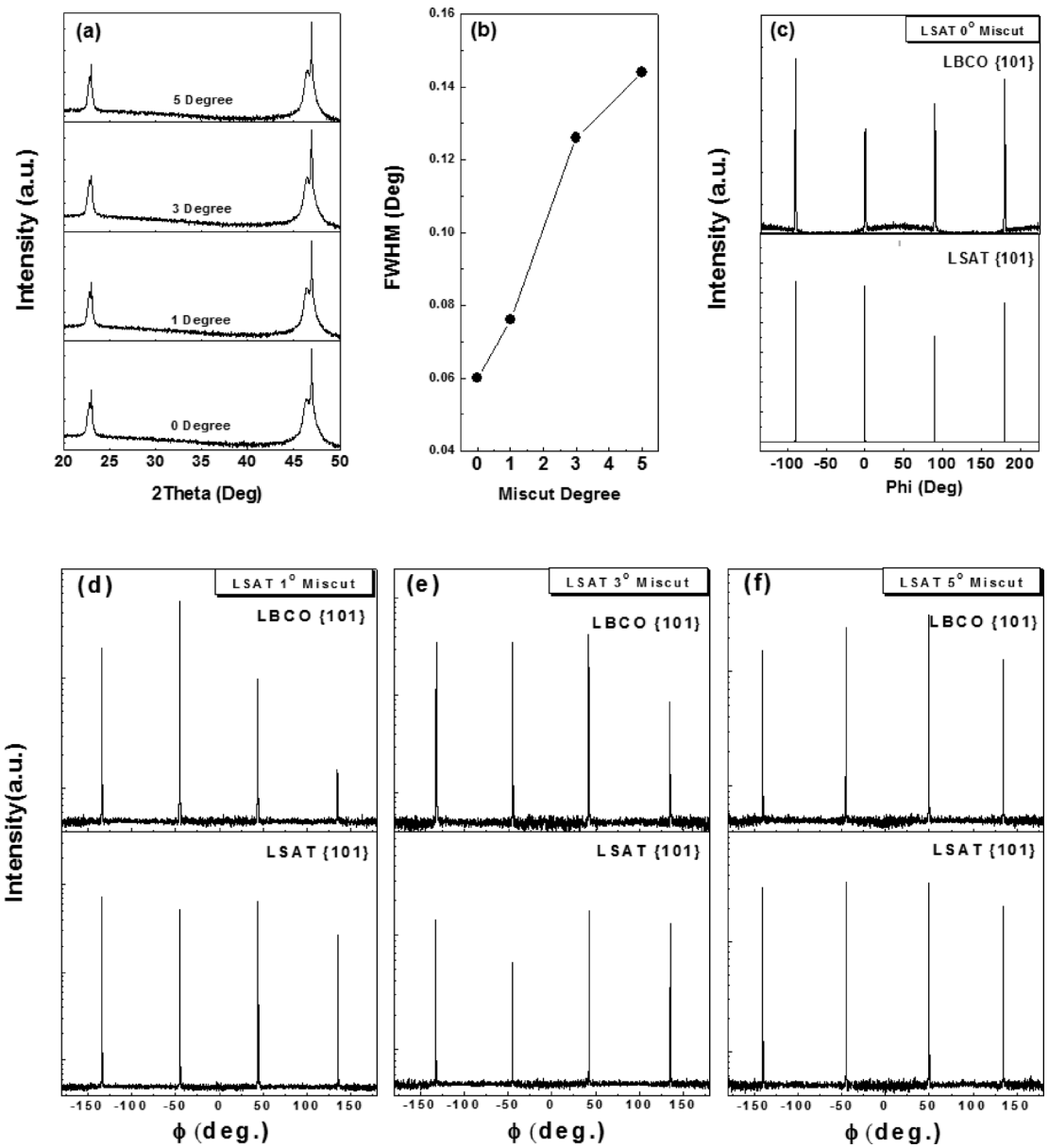

Fig. 1 XRD patterns of (a) θ–2θ; (b) rocking curves; (c)–(f) ϕ scans of LBCO films on vicinal LSAT substrates with various miscut angles of 0°, 1°, 3° and 5°.

deposition system is pumped down to 1×10^{-8} Torr. The growth condition was selected as being under an oxygen pressure of 250 mTorr at 800 °C with a laser energy density of about 2.0 J cm^{-2} at 5 Hz. After finishing the growth of the LBCO thin films, they were annealed at 800 °C for 15 min in pure oxygen (400 Torr), then slowly cooled down to room temperature at the rate of 5 °C min^{-1}. The thickness of the LBCO is of the order of nm. The phase structure, crystalline quality and interface relationship of the LBCO thin films were characterized using high-resolution X-ray diffraction (HRXRD) using a PANalytical X'Per MRD. The magnetic properties of the LBCO thin films were systematically studied using a Quantum Design Physical Property (PPMS-9) measurement system at different temperatures in the range of 10 K to 300 K.

Results and discussion

The crystalline quality of the LBCO thin films was characterized using XRD θ–2θ scans, rocking curves, ϕ scans and reciprocal space mappings (RSMs). Fig. 1(a) shows typical θ–2θ scanning patterns of the LBCO thin films on (001) vicinal LSAT substrates with various miscut angles of 0°, 1°, 3° and 5°. It can be seen that only (00l) peaks in the θ–2θ scan can be found for all the films, revealing that the LBCO thin films are c-axis oriented with no other impurities or phases. The rocking curve measurements from the (001) reflections for the films show that the Full Width of Half Maximum (FWHM) increases with the increase in the miscut angle, as shown in Fig. 1(b). The maximum FWHM is only ~0.15° for the LBCO films on 5° miscut angle substrates, indicating that all the LBCO films have an excellent crystalline quality. To understand the in-plane interface relationship between the LBCO films and the LSAT substrates with various miscut angles, the ϕ scan measurements have been performed, as shown in Fig. 1(c)–(f). The four-fold symmetry and sharp peaks in the ϕ scan patterns of the LBCO films on LSAT substrates with miscut angles of 0°, 1°, 3° and 5° further indicate that all the films have excellent crystalline qualities and epitaxial natures. Based on the data of the ϕ scans, the orientation relationship between the LBCO films and the LSAT substrates is determined to be $[100]_{LBCO}//[100]_{LSAT}$ and $(001)_{LBCO}//(001)_{LSAT}$.

More detailed microstructural information about the epitaxial thin films can be achieved using RSM technology, which is a very effective method in X-ray diffraction studies. The crystallographic evolution and the anisotropic in-plane interface strain of LBCO films on various surface-step-terraces have been measured using the RSMs taken from around the asymmetric (103) and (013) reflections of the LBCO films and LSAT substrates. The substrate miscut angle (SMA) direction along one of the in-plane axes (a or b) was

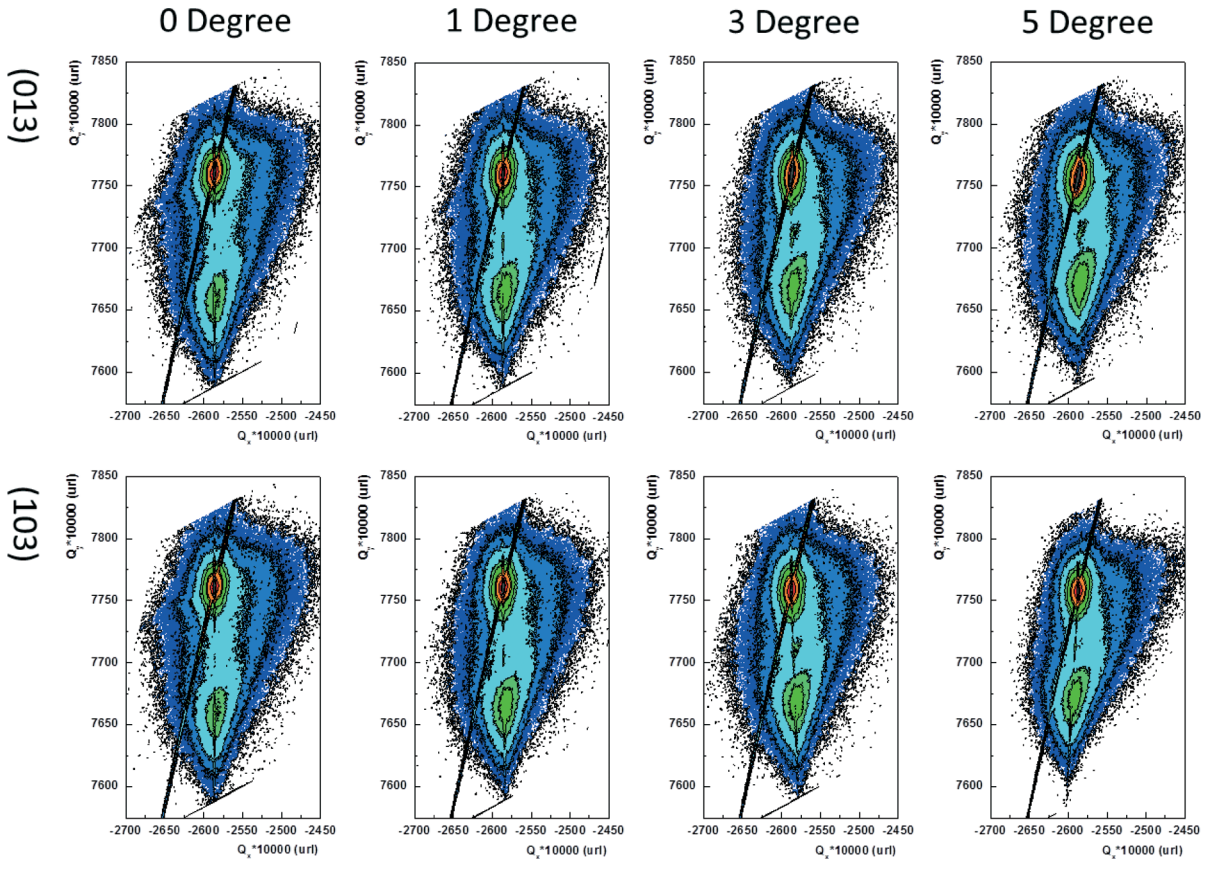

Fig. 2 Reciprocal space mappings taken from around the (103) and (013) reflections for the LBCO films on LSAT substrates with various miscut angles of 0°, 1°, 3° and 5°.

defined as the [100] direction. On the contrary, the direction defined as [010] is perpendicular to the SMA direction. Fig. 2 shows the asymmetric RSMs taken from around the (103) and (013) reflections of the LBCO films and various miscut LSAT substrates. First, the RSMs taken from around the (103) reflections along the [100] direction (the SMA direction) have been measured, in which we defined ϕ to be 0°. Then, the RSMs of (013) along the [010] direction were measured using the same method, but ϕ has been rotated by 90°. Therefore, the in-plane (*a* and *b*) and out-of-plane (*c*) lattice parameters of the LBCO films on various LSAT substrate surface-step-terraces have been calculated, as shown in Table 1. The in-plane (*b*) and the out-of-plane (*c*) lattice parameters for the four samples change very little, and these changes are within the error range. The in-plane lattice parameters (*a*) along the SMA direction of the LBCO film on the 1° and 3° LSAT miscut substrates have almost same value. The two LBCO films on the 1° and 3° LSAT miscut substrates have almost the same compressive strain of 0.4% along the [100] and [010] directions, which is a little larger than the 0.3% seen on 0° miscut LSAT substrates. However, it is worth noting that a significant decrease can be found for the lattice parameter *a* of the LBCO films on the 5° miscut angle substrates, which have a relatively larger compressive strain of 0.8% compared to the other three samples. To understand why the lattice parameter *a* (3.856 Å) of the films on the 5° miscut angle substrates is less than that of the other LSAT substrates, further research is underway.

Table 1 The in-plane (*a* and *b*) and out-of-plane (c) lattice parameters for the LBCO films on LSAT substrates with various miscut angles of 0°, 1°, 3° and 5°. The substrate miscut angle direction is along the in-plane *a* axis or the [100] direction

	Lattice parameters			Strain along	Strain along
Materials	*a* (100)	*b* (010)	*c* (001)	[100]	[010]
LBCO bulk	3.886				
LBCO on 0° LSAT	3.873	3.873r	3.916	0.3%	0.3%
LBCO on 1° LSAT	3.870	3.872	3.914	0.4%	0.4%
LBCO on 3° LSAT	3.869	3.873	3.912	0.4%	0.4%
LBCO on 5° LSAT	3.856	3.870	3.909	0.8%	0.4%

In order to investigate the possible anisotropy of the in-plane magnetic properties of the LBCO films on various surface-step-terraces, the magnetic moments along the [100] direction ($M_{//}$) and the [010] direction ($M_{\perp}$) were measured using a physical properties measurement system at different temperatures. Fig. 3 shows the temperature dependence of the magnetic moments (field-cooled or ZF measurements) in the temperature range from 30 K to 300 K along the $M_{//}$ direction and $M_{\perp}$direction for all the LBCO films on various surface-step-terraces. In our previous studies, the anisotropic in-plane strain field could significantly induce anisotropic

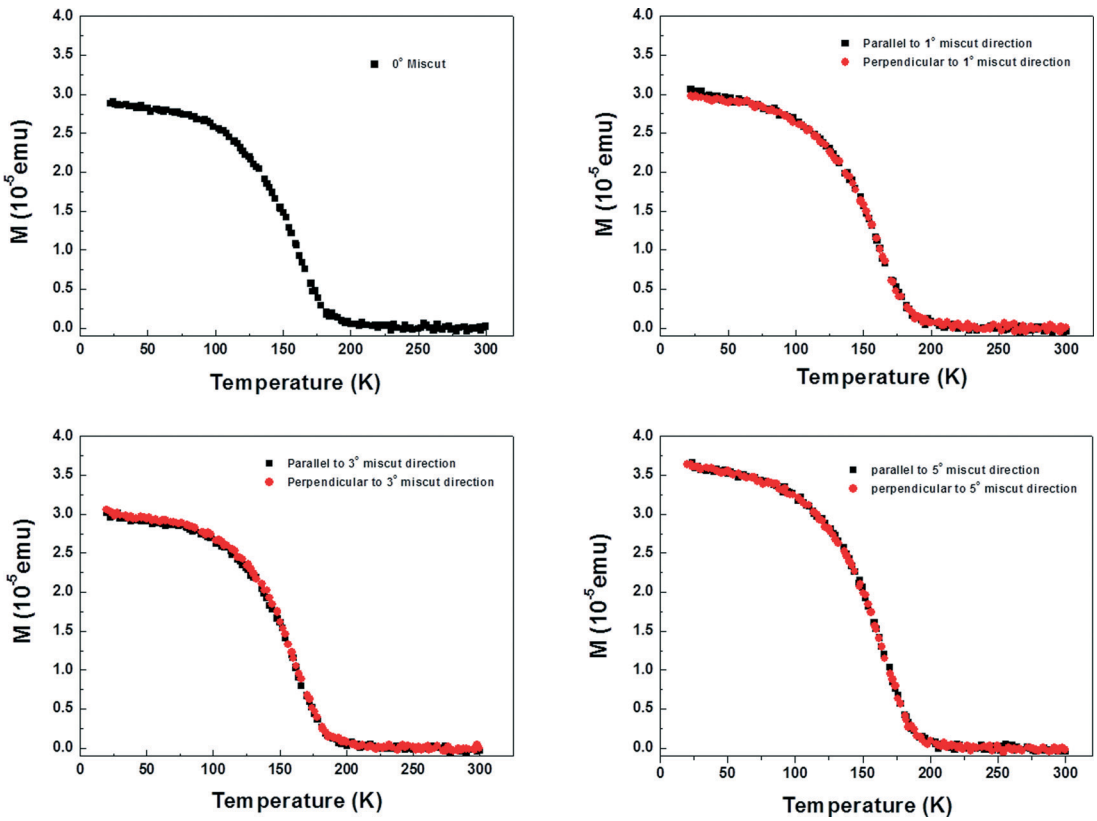

Fig. 3 The anisotropy of the in-plane magnetic properties of the LBCO films on LSAT substrates with various miscut angles of 0°, 1°, 3° and 5° under an applied magnetic field of 500 Oe, along the [100] and [010] directions.

resistance.[23,26] Here the magnetic moments along the $M_{//}$ direction and $M_{\perp}$ direction are almost unchanged for the LBCO films on LSAT substrates with miscut angles of 0°, 1°, and 3°. It is very easy to understand that all three samples have almost the same strain state along the $M_{//}$ direction and $M_{\perp}$ direction. However, for the LBCO film on substrates with a 5° miscut angle, the anisotropy strain states were obtained, for which the in-plane anisotropy magnetic properties haven't been found.

Furthermore, the SMA influence on the magnetic moments of the LBCO films has been studied. The temperature dependence of the field cooled (FC) magnetic moment measurements of the LBCO films on the LSAT substrates with various SMAs of 0°, 1°, 3° and 5° under an applied field of 500 Oe along the in-plane direction is shown in Fig. 4(a). The paramagnetic-to-ferromagnetic transition temperature (T_c) values, T_c = ~188 K, are higher than that of the LBCO bulk material's value of 175 K, which may result from the increasing hole density or destruction of the oxygen-hopping induced by oxygen deficiency.[35,36] Moreover, the T_c values of the LBCO thin films show almost no change, and are not influenced by the strain from the LSAT miscut substrates. However, the magnetic moments are highly dependent on the SMA. The LBCO film on the 5° LSAT miscut substrate exhibits the largest magnetic moment, followed by the LBCO films on the 3° and 1° substrates. The LBCO film on the 0° substrate shows the minimum magnetic moment. In order to further study the SMA dependent magnetic properties, the *M–H* hysteresis loops have also been measured. As shown in Fig. 4(b), the same SMA dependent magnetic phenomenon can be seen in the magnetic field dependence of the magnetic moment (m) at 20 K. These phenomena are probably due to the fact that the compressive strain from the miscut sample induces the shortening of the bond length between Co–O–Co, making the double exchange easier and increasing the magnetic moment. The compressive strain in the miscut substrate increases with the increase of the SMA. Thus, the magnetic moment increases with the increase of the SMA and the LBCO film on the 5° LSAT miscut substrate has the largest magnetic moment. Moreover, it can be clearly seen that each loop is a combination of two hysteresis loops, which is also found in our previous studies. The combined loop should be attributed to the nanoscale-ordered and disordered LBCO phases in the film. Meanwhile, the coercive field decreases as the SMA increases, which should be caused by the increase of in-plane compressive strain. It is known that the coercive fields for the disordered phase and the nanoscale-ordered LBCO bulk material are about 0.8 kOe and 4.2 kOe, respectively.[18] The strain can significantly affect the nanoscale-ordered and disordered phase composition. Large strain will make the disordered phase increase. On the contrary, small strain will induce an increase of the nanoscale-ordered phase. This phenomenon can be used to explain the reason why the coercive field decreases as the compressive strain increases. Overall, substrate surface treatment by changing the miscut angles can be thought of as an effective method to tune/control the magnetic properties of $LaBaCo_2O_{5.5+\delta}$ films.

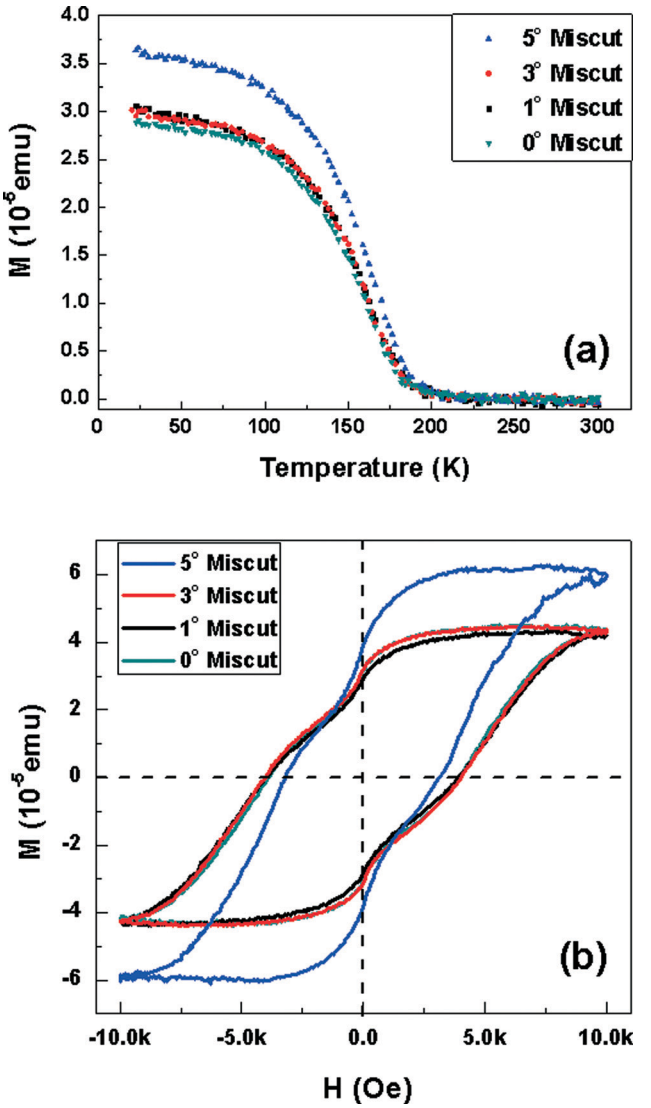

Fig. 4 Surface miscut angle dependent magnetic properties of the LBCO films on LSAT substrates with various miscut angles of 0°, 1°, 3° and 5°. (a) Temperature dependent magnetic moments (field cooled measurements) ranging from 20 K to 300 K under the applied magnetic field of 500 Oe; (b) *M–H* hysteresis loops at 20 K under the applied magnetic field of 1.0*T*.

Conclusion

Epitaxial LBCO films were grown on vicinal LSAT substrates with SMAs of 0°, 1°, 3° and 5° using pulsed laser deposition technology. All the LBCO films have a high crystalline quality with a maximum FWHM of ~0.15°. Reciprocal space mapping technology has been used to detect the strain relaxation behavior, revealing that the SMA can significantly affect the strain states in the LBCO films. Moreover, the different strain states can further tune the magnetic properties. Larger compressive strain along the in-plane direction can induce higher

magnetic moments and smaller coercive fields. Overall, the substrate surface-step-terrace can be used to as an effective technology to tune/control the magnetic properties of epitaxial LBCO films and related cobalt oxide films.

Acknowledgements

This research was supported by the Natural Science Foundation of China (No. 51202185 and 51390472), National "973" projects of China (No. 2015CB654903), the 111 Project of China (B14040), China Postdoctoral Science Fundation (No. 2015M572554), the National Science Foundation under NSF-NIRT-0709293, the Department of Energy under DE-FE0003780, and the State of Texas through the Texas Center for Superconductivity at the University of Houston.

References

1 G. C. Xiong, Q. Li, H. L. Ju, S. N. Mao, L. Senapati, X. X. Xi, R. L. Greene and T. Venkatesan, *Appl. Phys. Lett.*, 1995, **66**, 1427–1429.
2 R. Y. Zhang, M. Liu, L. Lu, S. B. Mi and H. Wang, *J. Mater. Chem. C*, 2015, **3**, 5598–5602.
3 J. Chang, E. Blackburn, A. T. Holme, N. B. Christensen, J. Larsen, J. Mesot, R. X. Liang, D. A. Bonn, W. N. Hardy and A. Watenphul, *Nat. Phys.*, 2012, **8**, 871–876.
4 I. Salaoru, T. Prodromakis, A. Khiat and C. Toumazou, *Appl. Phys. Lett.*, 2013, **102**, 013506.
5 Z. T. Xu, K. J. Jin, L. Gu, Y. L. Jin, C. Ge, C. Wang, H. Z. Guo, H. B. Lu, R. Q. Zhao and G. Z. Yang, *Small*, 2012, **8**, 1279–1284.
6 A. J. Jacobson, *Chem. Mater.*, 2010, **22**, 660–674.
7 Y. M. L. Yang, A. J. Jacobson, C. L. Chen, G. P. Chen, K. D. Ross and C. W. Chu, *Appl. Phys. Lett.*, 2001, **79**, 776–778.
8 G. P. Luo, Y. S. Wang, S. Y. Chen, A. K. Heilman, C. L. Chen, C. W. Chu and Y. Liou, *Appl. Phys. Lett.*, 2000, **76**, 1908–1910.
9 Y. M. Kim, J. He, M. D. Biegalski, H. Ambaye, V. Lauter, H. M. Christen, S. T. Pantelides, S. J. Pennycook, S. V. Kalimin and A. Y. Borisevich, *Nat. Mater.*, 2012, **11**, 888–894.
10 A. A. Taskin, A. N. Lavrov and A. Yoichi, *Appl. Phys. Lett.*, 2005, **86**, 091910.
11 G. Kim, S. Wang, A. J. Jacobson, C. L. Chen, L. Reimus, P. Brodersen and C. A. Mims, *Appl. Phys. Lett.*, 2006, **88**, 024103.
12 G. Kim, S. Wang, A. J. Jacobson, L. Reimus, P. Brodersen and C. A. Mims, *J. Mater. Chem.*, 2007, **17**, 2500.
13 Z. Yuan, J. Liu, C. L. Chen, C. H. Wang, X. G. Luo, X. H. Chen, G. T. Kim, D. X. Huang, S. S. Wang, A. J. Jacobson and W. Donner, *Appl. Phys. Lett.*, 2007, **90**, 212111.
14 A. Aguadero, D. Perez-Coll, J. A. Alonso, S. J. Skinner and J. Kilner, *Chem. Mater.*, 2012, **24**, 2655–2663.
15 F. Fauth, E. Suard and V. Caignaert, *Phys. Rev. B: Condens. Matter Mater. Phys.*, 2002, **65**, 060401.
16 T. Nakajima, M. Ichihara and Y. Ueda, *J. Phys. Soc. Jpn.*, 2005, **74**, 1572–1577.
17 A. K. Kundu, E.-L. Rautama, P. Boullay, V. Caignaert, V. Pralong and B. Raveau, *Phys. Rev. B: Condens. Matter Mater. Phys.*, 2007, **76**, 184432.
18 E. L. Rautama, P. Boullay, A. K. Kundu, V. Caignaert, V. Pralong, M. Karppinen and B. Raveau, *Chem. Mater.*, 2008, **20**, 2742–2750.
19 E. L. Rautama, V. Caignaert, P. Boullay, A. K. Kundu, V. Pralong, M. Karppinen, C. Ritter and B. Raveau, *Chem. Mater.*, 2009, **21**, 102–109.
20 J. Liu, M. Liu, G. Collins, C. L. Chen, X. N. Jiang, W. Q. Gong, A. J. Jacobson, J. He, J. C. Jiang and E. I. Meletis, *Chem. Mater.*, 2010, **22**, 799–802.
21 M. Liu, J. Liu, G. Collins, C. R. Ma, C. L. Chen, J. He, J. C. Jiang, E. I. Meletis, A. J. Jacobson and Q. Y. Zhang, *Appl. Phys. Lett.*, 2010, **96**, 132106.
22 C. R. Ma, M. Liu, G. Collins, H. B. Wang, S. Y. Bao, X. Xu, E. Enriquez, C. L. Chen, Y. Lin and M. H. Whangbo, *ACS Appl. Mater. Interfaces*, 2013, **5**, 451–455.
23 M. Liu, C. R. Ma, J. Liu, G. Collins, C. L. Chen, J. He, J. C. Jiang, E. I. Meletis, L. Sun, A. J. Jacobson and M. H. Whangbo, *ACS Appl. Mater. Interfaces*, 2012, **4**, 5524–5528.
24 J. He, J. C. Jiang, J. Liu, M. Liu, G. Collins, C. R. Ma, C. L. Chen and E. I. Meletis, *Thin Solid Films*, 2011, **519**, 4371–4376.
25 M. Liu, C. Ma, G. Collins, J. Liu, C. Chen, C. Dai, Y. Lin, L. Shui, F. Xiang, H. Wang, J. He, J. Jiang, E. I. Meletis and M. W. Cole, *ACS Appl. Mater. Interfaces*, 2012, **4**, 5761–5765.
26 J. Chakhalian, A. J. Millis and J. Rondinelli, *Nat. Mater.*, 2012, **11**, 92–94.
27 T. Yajima, Y. Hikita, M. Minohara, C. Bell, J. A. Mundy, L. F. Kourkoutis, D. A. Muller, H. Kumigashira, M. Oshima and H. Y. Hwang, *Nat. Commun.*, 2015, **6**, 6759.
28 C. R. Ma, M. Liu, J. Liu, G. Collins, Y. M. Zhang, H. B. Wang, C. L. Chen, Y. Lin, J. He, J. C. Jiang, E. I. Meletis and A. J. Jacobson, *ACS Appl. Mater. Interfaces*, 2014, **6**, 2540–2545.
29 Q. Zou, M. Liu, G. Q. Wang, H. L. Lu, T. Z. Yang, H. M. Guo, C. R. Ma, X. Xu, M. H. Zhang, J. C. Jiang, E. I. Meletis, Y. Lin and H. J. Gao, *ACS Appl. Mater. Interfaces*, 2014, **6**, 6704–6708.
30 J. C. Jiang, Y. Lin, C. L. Chen, C. W. Chu and E. I. Meletis, *J. Appl. Phys.*, 2002, **91**, 3188–3192.
31 M. Liu, Q. Zou, C. R. Ma, G. Collins, S. B. Mi, C. L. Jia, H. M. Guo, H. J. Gao and C. L. Chen, *ACS Appl. Mater. Interfaces*, 2015, **6**, 8526–8530.
32 M. P. Singh, K. D. Truong, P. Fournier, P. Rauwel, E. Rauwel, L. P. Carignan and D. Menard, *J. Magn. Magn. Mater.*, 2009, **321**, 1743–1747.
33 M. P. Singh, K. D. Truong, P. Fournier, P. Rauwel, E. Rauwel, L. P. Carignan and D. Menard, *Appl. Phys. Lett.*, 2008, **92**, 112505.
34 C. R. Ma, M. Liu, C. L. Chen, Y. Lin, Y. R. Li, J. S. Horwitz, J. C. Jiang, E. I. Meletis and Q. Y. Zhang, *Sci. Rep.*, 2013, **3**, 3092.
35 J. Kwon, Y. Gim, Y. Fan, M. F. Hundley, J. M. Roper, P. N. Arendt and Q. X. Jia, *J. Appl. Phys.*, 2003, **94**, 7670–7674.
36 C. K. Xie, J. I. Budnick and B. O. Wells, *Appl. Phys. Lett.*, 2007, **91**, 172509.

